THE FASEB JOURNAL • RESEARCH • www.fasebj.org

Oligomerization of equilibrative nucleoside transporters: a novel regulatory and functional mechanism involving PKC and PP1

Natalia Grañe-Boladeras,[*,†,‡,1] Declan Williams,[§] Zlatina Tarmakova,[*] Katarina Stevanovic,[*] Linda A. Villani,[¶] Pedram Mehrabi,[¶] K. W. Michael Siu,[§] Marçal Pastor-Anglada,[†,‡] and Imogen R. Coe[*]

[*]Department of Chemistry and Biology, Ryerson University, Toronto, Ontario, Canada; [†]Department of Biochemistry and Molecular Biomedicine, Institute of Biomedicine, University of Barcelona, Barcelona, Spain; [‡]National Biomedical Research Institute of Liver and Gastrointestinal Diseases, Barcelona, Spain; and [§]Department of Chemistry and [¶]Department of Biology, York University, Toronto, Ontario, Canada

ABSTRACT: Equilibrative nucleoside transporters (ENTs) translocate nucleosides and nucleobases across plasma membranes, as well as a variety of anti-cancer, -viral, and -parasite nucleoside analogs. They are also key members of the purinome complex and regulate the protective and anti-inflammatory effects of adenosine. Despite their important role, little is known about the mechanisms involved in their regulation. We conducted membrane yeast 2-hybrid and coimmunoprecipitation studies and identified, for the first time to our knowledge, the existence of protein–protein interactions between human ENT1 and ENT2 (hENT1 and hENT2) proteins in human cells and the formation of hetero- and homo-oligomers at the plasma membrane and the submembrane region. The use of NanoLuc Binary Technology allowed us to analyze changes in the oligomeric status of hENT1 and hENT2 and how they rapidly modify the uptake profile for nucleosides and nucleobases and allow cells to respond promptly to external signals or changes in the extracellular environment. These changes in hENTs oligomerization are triggered by PKC activation and subsequent action of protein phosphatase 1.—Grañe-Boladeras, N., Williams, D., Tarmakova, Z., Stevanovic, K., Villani, L. A., Mehrabi, P., Siu, K. W. M., Pastor-Anglada, M., Coe, I. R. Oligomerization of equilibrative nucleoside transporters: a novel regulatory and functional mechanism involving PKC and PP1. FASEB J. 33, 3841–3850 (2019). www.fasebj.org

KEY WORDS: MYTH · NanoBiT · hENT1 · hENT2 · adenosine

Equilibrative nucleoside transporters (ENTs), encoded by the SLC29 gene family, are bidirectional passive nucleoside transporters, primarily located at the plasma membrane, which can translocate their substrates in either direction down the substrate concentration gradient (1). ENT substrates include nucleosides and nucleobases, such as adenosine and hypoxanthine (Hx), as well as nucleoside-derived drugs, used in a variety of anti-cancer, -viral, and -parasite therapies. A total of 4 members of the ENT family have been identified in mammals to date (ENT1–ENT4) although ENT1 and ENT2 are the major contributors to nucleoside transport across the plasma membrane in many tissues (2, 3).

ENTs are also key members of the purinome complex and regulate the purinergic signaling in the CNS, as well as in the cardiovascular and renal systems, by modulating adenosine levels inside and outside the cell (2, 4). In many pathophysiological conditions, such as myocardial ischemia, inflammation, or diabetic nephropathy, ENTs become therapeutic targets, frequently inhibited with treatments, such as dipyridamole or dilazep, to reduce the adenosine reuptake and promote the protective and anti-inflammatory effects of this bioactive nucleoside (5–7). Despite their important role in cell physiology and pharmacology, the mechanisms implicated in their regulation, particularly at the post-translational level, are not well known.

In this regard, several studies have either suggested or demonstrated that human ENT (hENT) function can be

ABBREVIATIONS: CID, collision-induced dissociation; CKII, casein kinase 2; Cl-Ado, chloroadenosine; ENT, equilibrative nucleoside transporter; ETD, electron transfer dissociation; HA, hemagglutinin; HEK-293, human embryonic kidney 293; hENT1, human equilibrative nucleoside transporter 1; hENT2, human equilibrative nucleoside transporter 2; His, histidine; Hx, hypoxanthine; LC, liquid chromatography; MS, mass spectrometry; MS/MS, tandem mass spectrometry; MYTH, membrane yeast 2 hybrid; NanoBiT, NanoLuc Binary Technology; PDD, phorbol 12,13-didecanoate; PP1, protein phosphatase 1; PPI, protein–protein interaction; TTM, tautomycin; Ubq, ubiquitin

[1] Correspondence: Department of Chemistry and Biology, Ryerson University, 350 Victoria St., Toronto, ON, Canada M5B 0A1. E-mail: nataliagrane@ryerson.ca

doi: 10.1096/fj.201800440RR
This article includes supplemental data. Please visit *http://www.fasebj.org* to obtain this information.

regulated by phosphorylation, glycosylation, ethanol, and calmodulin binding (8–11) and even proposed oligomerization of ENT1 (9). However, there are still many unsolved gaps in the bigger picture of ENT regulation. Although there is recent evidence suggesting that concentrative nucleoside transporter proteins can form homotrimers from prokaryotes to humans (12, 13), how ENTs are structurally organized is not known. Thus, there is no evidence, to date, that would suggest complex quaternary structures of ENTs and the functional implications of those.

In this study, we confirm protein–protein interactions (PPIs) between hENT1 and hENT2 and the formation of homo- and heteromers at the plasma membrane and submembrane regions. We describe the regulatory effects of the changes in the oligomeric status of ENTs on the capacity to internalize adenosine and Hx. Our work also elaborates on the direct phosphorylation of hENT1 and hENT2 by PKA, PKC, and casein kinase 2 (CKII) and the involvement of PKC activation and subsequent dephosphorylation of hENT2 by protein phosphatase 1 (PP1) in the regulation of hENT oligomerization.

MATERIALS AND METHODS

Cell culture, DNA transfection, and treatments

Human embryonic kidney 293 (HEK-293; CRL-1573; American Type Culture Collection, Manassas, VA, USA) cells were maintained in proliferative conditions in DMEM with 4.5 mg/ml glucose and supplemented with 10% (v/v) fetal bovine serum (Thermo Fisher Scientific, Waltham, MA, USA) at 37°C in a humidified incubator and a 5% CO_2 atmosphere. This cell line was certified to be mycoplasma free by an external agency (DDC Medical; Thermo Fisher Scientific). When indicated, cells were transiently transfected using Lipofectamine 3000 (Thermo Fisher Scientific), according to the manufacturer's instructions, obtaining transfection efficiencies of ~60–70%. Protein extraction, confocal microscopy, and nucleoside transport assays were carried out 36 h after transfection, and knockdown experiments were analyzed at 72 h post-transfection. In this study, DNA constructs were used to express hemagglutinin (HA)- and Flag-tagged hENT1 and hENT2 proteins—all of them previously used in our laboratory (9, 14)—as well as a set of predesigned commercial short hairpin RNA constructs to knock down hENT2 (HSH008931; Genecopoeia, Rockville, MD, USA). When indicated, cells were treated with the PKC activator phorbol 12,13-didecanoate (PDD; MilliporeSigma, Burlington, MA, USA), its inactive form 4α-PDD (MilliporeSigma), or the PP1 inhibitor tautomycin (TTM; Santa Cruz Biotechnology, Dallas, TX, USA), all 3 at a concentration of 500 nM for 10 min.

Membrane yeast 2-hybrid and coimmunoprecipitation

The membrane yeast 2-hybrid (MYTH) technique is a novel, high-throughput approach that adapts the principle of split ubiquitin (Ubq) to identify PPIs between transmembrane proteins (baits) and putative partners (preys) (15). Following the protocol described in Snider *et al.* (15),.hENT1 and hENT2 cDNAs were cloned into the prey (pPR3-N) and bait (pTLB1) vectors, both kindly donated by Dr. Igor Stagljar (University of Toronto, Toronto, ON, Canada). Each bait vector was then transformed together with one of the prey, as well as a positive and a negative prey vector, into NMY51 yeast strain. Cells were then plated on selective media plates (SD-WLAH) and incubated at 30°C for 3–4 d. Yeast cells growing on those selective plates confirmed the existence of the PPI between the prey and the bait hENT proteins expressed in yeast.

To confirm PPI among hENTs in human cells, HEK-293 cells were transiently transfected with hENT1-HA and hENT2-HA constructs as baits alone or together, with Flag-hENT1, Flag-hENT2, or negative control Flag-human LA (hLa) protein constructs as preys. At 36 h post-transfection, we extracted total protein using Nonidet P-40 lysis buffer [50 mM Tris-HCl, pH 8, 150 mM NaCl, 1% (v/v) Nonidet P-40, 5 mM $Na_4P_2O_7$, 50 mM NaF, 1 mM Na_3VO_4, and protease inhibitor cocktail (Complete Mini); Roche, Basel, Switzerland]. Protein extracts were quantified using the Bradford Protein Assay Kit (Bio-Rad, Hercules, CA, USA) and incubated with HA-affinity columns from Pierce HA Tag Immunoprecipitation/Coimmunoprecipitation Kit (Thermo Fisher Scientific), following the manufacturer's protocol. Eluted proteins were separated in Bolt 4–12% Bis-Tris Plus Gels (Thermo Fisher Scientific) by electrophoresis, following the manufacturer's instructions, and transferred to nitrocellulose membranes (Bio-Rad). Following incubation with anti-Flag (MilliporeSigma), anti-ENT1 rabbit polyclonal (Abcam, Cambridge, MA, USA), or rabbit monoclonal anti-ENT2 antibody (Abcam), proteins were detected using a secondary antibody conjugated to horseradish peroxidase and an ECL Detection Kit (Thermo Fisher Scientific).

Confocal microscopy

To determine the subcellular localization of hENT1 and -2 proteins and their spatial proximity within cells, immunocytochemistry and confocal microscopy assays were conducted with HEK-293 cells cultured on glass coverslips expressing hENT2-HA, alone or together with Flag-hENT1. Cells were treated with either 4α-PDD as a control or PDD to activate PKC, quickly rinsed with PBS, incubated for 15 min in 3% (w/v) paraformaldehyde in PBS, and rinsed 3 times in PBS. When indicated, samples were permeabilized with 0.1% Triton X-100 in PBS and rinsed 3 times in PBS. Samples were then incubated with 10% (v/v) fetal bovine serum in PBS for 30 min, incubated with anti-HA (Roche) and anti-Flag (MilliporeSigma) for 1 h at room temperature, rinsed 3 times with PBS, incubated with secondary antibodies Alexa 555 donkey anti-mouse and Alexa 488 donkey anti-rat (Thermo Fisher Scientific), rinsed 3 times with PBS, and mounted on slides using aqua-based mounting medium (MP Biomedicals, Santa Ana, CA, USA). Images were obtained using the Olympus (Tokyo, Japan) Fluoview 300 confocal microscope and analyzed with Olympus Fluoview 300 imaging software under blind observation to preserve an objective perception. All of the confocal images show a single and representative section of a *z* series taken through the entire cell.

Phosphorylation analysis of hENTs by *in silico* and *in vitro* assays

The hENT intracellular loop between transmembrane domains 6 and 7 is the largest intracellular region accessible to other cytoplasmic proteins and most likely to be phosphorylated by kinases. An *in silico* analysis of the potential phosphosites within hENT1 and hENT2 intracellular loops and the potential kinases involved were first conducted. This analysis was performed using NetPhosK software (16). Two customized constructs were then purchased from DNA 2.0 containing hENT1 and hENT2 loops, preceded by 6 histidine (His) residues and a Ubq sequence, which included a thrombin cleavage site. Plasmids were transformed into *Escherichia coli* DH5α bacteria and scaled up to 1 l M9 minimal medium. When the bacterial culture reached an optical density 600 nm = 0.7, 1 mM isopropyl β-D-1-thiogalactopyranoside was added to induce protein expression. Bacteria were

induced at 37°C for 2 h and then spun in a centrifuge (Thermo Fisher Scientific) at 7000 *g* for 20 min.; the resulting pellets were resuspended in 30 ml T300 and passed through a French press (5 times) to lyse bacteria and release the protein. Unbroken cell debris was then spun in a centrifuge at 10,000 *g* for 20 min. His–Ubq-tagged peptides were extracted from the supernatant using standard nickel affinity chromatography methods. In brief, following preparation of the column with 50 mM $NiCl_2$, protein was bound at a rate of 2 ml/min. The column was then washed at a rate of 5 ml/min, first with 100 ml T300 and then with 100 ml T300 buffer, supplemented with 10 mM imidazole. Bound protein was eluted from the column using 50 ml T300 buffer, supplemented with EDTA 20 mM. The presence of the peptide was confirmed using a 10% SDS gel and Coomassie blue staining. The 50 ml sample was then concentrated at 4000 *g* to 4 ml using Microcon YM-3 columns (MilliporeSigma) and subjected to further purification by FPLC using a Sephadex S-100 16/60 column (GE Biosciences, Chicago, IL, USA). The resulting elution fraction was concentrated to 5 ml using Microcon (MilliporeSigma) YM-3 columns.

In vitro phosphorylation studies were conducted using 10 μg of the hENT-loop peptide or histone H1 as positive control. Peptides were treated with PKC (0.02 U), PKA (2500 U), or CKII (500 U) and γ-[^{32}P]-ATP (0.25 mCi/ml; for autoradiography) or nonradiolabeled ATP for mass spectrometry (MS). Following a 2-h incubation at 30°C, samples were mixed with an appropriate volume of protein loading buffer and boiled at 90°C for 10 min. Protein samples were separated by 10% SDS-PAGE for 3.5 h at 200 V. Following separation, 16 kDa bands, representing phosphorylated or nonphosphorylated hENT peptides, were visualized using Coomassie blue stain. Gels containing radiolabeled protein were dried and subjected to autoradiography using standard imaging film in cassettes lined with a [^{32}P] intensifying screen for 1 h at room temperature or overnight at −80°C.

Phosphorylation analysis by MS

Dried Ubq-hENT chimera protein samples were dissolved in 100 μl of 100 mM NH_4HCO_3 and denatured at 65°C for 10 min. Any cysteine residues present were reduced with 5 mM DTT for 30 min at 65°C and then derivatized with 10 mM iodoacetamide for 30 min at room temperature in the dark. Each sample was then treated with 1 μg porcine trypsin (Promega, Madison, WI, USA), incubated at 37°C for 16 h, and then dried in a centrifugal concentrator (MilliporeSigma).

Tryptic peptides were purified using C18 ZipTips (MilliporeSigma), dried in a centrifugal concentrator, then suspended in water containing 0.1% (v/v) formic acid, and subjected to Nanoflow High-Performance Liquid Chromatorgraphy Tandem MS (LC-MS/MS). Chromatographic separation was carried out on a cHiPLC-Nanoflex system, supplied with mobile phase by a NanoLC Ultra 2-Dimensional High-Performance LC Pump (AB Sciex, Framingham, MA, USA), and mass spectra were acquired on an Orbitrap Elite Mass Spectrometer equipped with electron transfer dissociation (ETD; Thermo Fisher Scientific). Samples were injected onto the chromatographic system by the autosampler and carried to a 0.05-mm long, 200-μm diameter trap column at 2 μl/min in aqueous 2% acetonitrile acidified with 0.1% formic acid. A 150-mm long, 75-μm diameter column was used for the chromatographic separation. The trap and column were both packed with 3 μm diameter C18 stationary phase with a pore size of 120 Å. A binary mobile-phase gradient was used, with mobile phases A and B containing 0.1% (v/v) formic acid in water and acetonitrile, respectively. The mobile phase B compositions over the gradient were the following: 2% at 0 min, 35% at 35 min, 80% at 35.5 min, 80% at 38.5 min, 2% at 39 min, and 2% at 55 min.

In the initial LC-MS/MS analysis, the mass range of the precursor ion scans was 400—1500 Th (Thomson), and precursors were selected for fragmentation on the basis of their signal intensity alone. Collision-induced dissociation (CID) was used to fragment these ions. The resulting data were interrogated for peptide sequences using the Sequest algorithm operated in Proteome Discoverer software (Thermo Fisher Scientific). The complete database of canonical and variant human protein sequences, downloaded from Uniprot (*https://www.uniprot.org/*) on April 24, 2013, was used for the search. The following parameters were applied to this and all subsequent searches: s/n threshold, 1.5; maximum missed cleavages, 1; precursor mass tolerance, 10 ppm; fragment mass tolerance, 0.8 Da; product ions considered, *b* and *y* for CID, *c* and *z* for ETD; weight of any product ion, 1; maximum modifications per peptide, 4; static modifications, carbamidomethyl cysteine; dynamic modifications, oxidation (M), phosphorylation (S,T,Y), deamidation (Q) (Supplemental Data). A decoy database search was used to assess the accuracy of peptide identifications, with a target false discovery rate of 0.01. This database contained 141,887 sequences with a total of 54,955,122 aa. Phosphopeptides of hENT1 and hENT2, identified in the search results, were specifically targeted in subsequent analyses to obtain more detailed MS/MS data.

An acquisition method featuring an inclusion list was added to analyze preferentially precursor ions with mass-to-charge ratio values corresponding to the previously identified hENT phosphopeptides using both CID and ETD. The samples were reanalyzed by LC-MS/MS with the targeted acquisition method, and the data searched for peptide-specific data with Sequest with the same settings used previously.

NanoBiT

The novel NanoLuc Binary Technology (NanoBiT) system (Promega) was used to quantify PPIs among hENTs in live cells. This technology is composed of 2 small subunits—large BiT and small BiT—that are fused to the proteins of interest. Once the target proteins interact within the cell, the subunits come together and form an active enzyme that generates bright luminescent signal. This technology allows real-time kinetic analysis in live cells and detection at low expression levels of the interacting proteins (17).

Following the manufacturer's instructions, hENT1 and -2 cDNAs were cloned into the N-term large and small BiT vectors. The transfection protocol was optimized and the constructs validated using the controls provided with the kit. Following the manufacturer's protocol, PPIs between hENT1–hENT1, hENT1–hENT2, and hENT2–hENT2 proteins were analyzed in HEK-293 cells. Each set of samples was treated with DMSO as a control, PDD as a PKC activator, TTM as a PP1 inhibitor, or PDD and TTM together and measured luminescence at 1-min intervals. Results were normalized to time = 0 min.

Nucleoside and nucleobase transport assays

Transport studies of endogenous hENTs on monolayer-cultured cells were carried out, as previously described (14), by exposing replicate cultures at room temperature to the appropriate H^3-labeled nucleoside or nucleobase (1 μM, 1 μCi/ml) in uptake buffer (5.4 mM KCl, 1.8 mM $CaCl_2$, 1.2 mM $MgSO_4$, 10 mM HEPES, and 137 mM choline chloride). Incubation was stopped after 10 s by washing the monolayers 3 times in cold uptake buffer supplemented with nitrobenzylthioinosine and dipyridamole. Cells were lysed in 2 M NaOH for 24 h at 4°C. Aliquots were taken to measure protein concentration (modified Lowry Protein Assay; Bio-Rad) and nucleoside uptake (standard liquid scintillation counting). Based on the individual contributions of hENT1 and hENT2 to the total uptake of chloroadenosine (Cl-Ado) and Hx (Supplemental Fig. S1), we considered total Cl-Ado uptake in HEK-293 cells to be mediated by hENT1 and total Hx uptake in HEK-293 cells to be mediated by hENT2.

RESULTS

hENT1 and hENT2 proteins interact and form homo- and heteromers in yeast and HEK-293 cells

We confirmed the existence of hENT1–hENT1, hENT2–hENT2, and hENT1–hENT2 PPI when expressed in yeast using the MYTH system (15). Our results (**Fig. 1*A***) showed that yeast colonies cotransformed with either hENT1-bait (left) or hENT2-bait (right) constructs, and hENT1-prey or hENT2-prey constructs were PPI positive and grew on selective medium.

To ensure hENT PPIs also occurred in mammalian cells, we coimmunoprecipitated HA (bait)- and Flag (prey)-tagged hENT1 and hENT2 proteins expressed in combinations of 2 in HEK-293 cells (Fig. 1*B*). Our results showed coimmunoprecipitation of hENT1–hENT1, hENT2–hENT2, and hENT1–hENT2 and suggested the formation of homo- and heteromers between hENTs in HEK-293 cells. We further investigated these results and corroborated the formation of heteromers between overexpressed HA-tagged hENT and endogenously expressed hENT proteins (Fig. 1*C*). Taken together, we confirmed the formation of homo- and heteromers between ENT1 and ENT2 in yeast and mammalian cells.

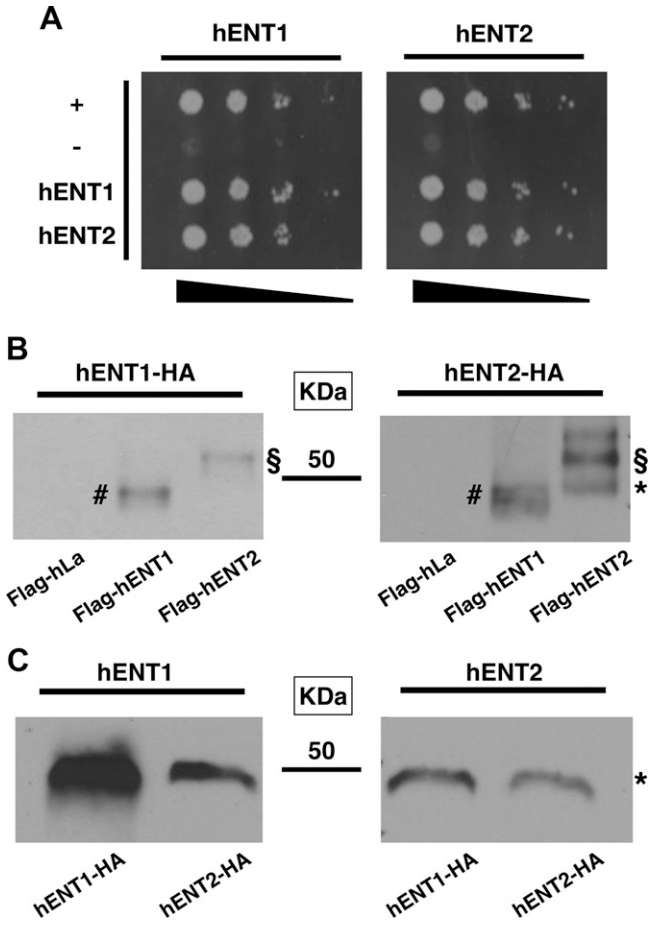

Figure 1. hENT1 and hENT2 form homo- and heteromers in yeast and HEK-293 cells. *A*) hENT1 (left)- and hENT2 (right)-bait MYTH constructs coexpressed with hENT1- and hENT2-prey constructs, as well as positive (+) and negative (−) prey controls in yeast. Yeast colonies grown in SD-WLAH-selective medium confirm positive PPI between the bait and the prey constructs. *B*) Coimmunoprecipitation of HA-tagged hENT1 (left) and hENT2 (right) proteins with Flag-tagged hLa (noninteracting cytosolic protein; negative control), hENT1, and hENT2. Proteins were expressed in combinations of 2 (a bait and a prey). Blots were probed against the Flag tag using anti-flag antibody from MilliporeSigma. Flag-hENT1 bands appear below the 50 kDa mark (#), whereas Flag-hENT2 shows 3 different bands: one below 50 kDa (∗), one above 50 kDa (§), and a third one of higher MW. *C*) Coimmunoprecipitation of endogenous hENT1 (left) and endogenous hENT2 (right) with HA-tagged hENT1 and hENT2. Blots were probed against hENT1 (left) and hENT2 (right) endogenous proteins using anti-hENT1 (rabbit polyclonal) and anti-hENT2 (rabbit monoclonal) antibodies. The endogenous hENT1 band coincides with one of the isoforms observed by Bicket and Coe (9), whereas the hENT2 band coincides with the lower band expressed in *B* (∗). For the 3 panels, these are representative images of $n = 3$.

PKC activation promotes traffic of hENT2 to the plasma membrane and its colocalization with hENT1

Based on our PPI results, we anticipated that hENT1 and hENT2 would be in close proximity within a cell for the interaction to occur. Surprisingly, confocal microscopy of HEK-293 cells, coexpressing both transporter proteins, revealed hENT1 present at the plasma membrane and hENT2 located at the submembrane region in basal conditions (**Fig. 2*A***). Previous studies described that PDD-dependent PKC activation increases hENT2 transport activity at the plasma membrane (18). Therefore, we predicted that PKC activation would promote traffic of hENT2 to the plasma membrane from the submembrane region. Indeed, we confirmed an increased presence of hENT2 at the plasma membrane after PKC activation (Fig. 2*A, B*) and subsequent colocalization of hENT2-HA and Flag-hENT1 (Fig. 2*A*). We further confirmed that PKC activation triggers hENT2-HA traffic to the plasma membrane (rather than internalizing hENT1 to the submembrane region) by repeating the confocal microscopy assays with and without permeabilization of the cells with detergent before the incubation with antibodies (Fig. 2*B*).

hENT1 and hENT2 are differentially phosphorylated by PKA and CKII *in vitro*

Previous data suggest that ENTs are regulated and putatively phosphorylated by several kinases, such as PKA, PKC, and CKII (2, 8, 19). Furthermore, our laboratory recently confirmed *in vitro* phosphorylation of hENT1 by PKA and possibly by PKC using radiolabeled γ-[^{32}P]-ATP (8), although the functional significance of this post-translational modification remains unclear. Hence, we hypothesized that PKC phosphorylates hENT2 and promotes its traffic to the plasma membrane after its PDD-induced activation.

In silico analysis of hENT1 and hENT2 intracellular loops (potential regulatory hub of ENTs) identified amino acids that could potentially be phosphorylated by PKA,

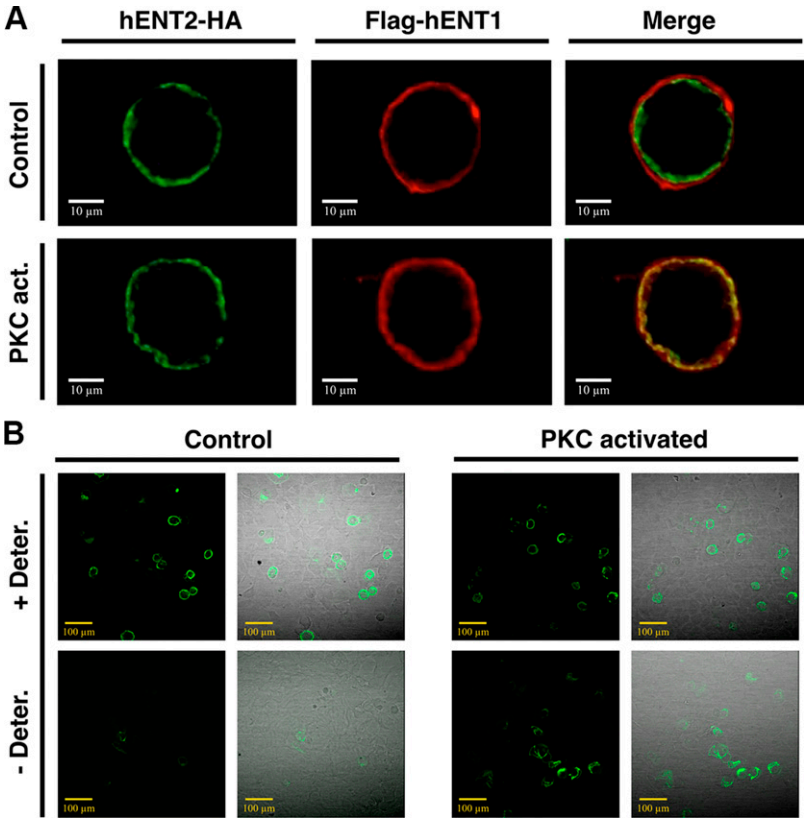

Figure 2. PKC activation leads to hENT2 redistribution from the submembrane region to the plasma membrane and colocalization with hENT1. *A*) Immunofluorescence confocal microscopy of HEK-293 cells coexpressing hENT2-HA (green) and Flag-hENT1 (red). Untreated cells (upper) express hENT2-HA at the submembrane region and Flag-hENT1 at the plasma membrane. PKC-activated (act.) cells (lower) express both Flag-hENT1 and hENT2-HA at the plasma membrane where they colocalize. Representative images of $n = 6$; original scale bars, 10 μm. *B*) Immunofluorescence confocal microscopy of HEK-293 expressing hENT2-HA with and without permeabilization [+/− detergent (Deter.)] before incubation with antibody. Control cells (left) show very little hENT2-HA at the plasma membrane, whereas PKC-activated cells (right) show higher presence compared with control. Representative images of $n = 3$; original scale bars, 100 μm.

PKC, or CKII (**Fig. 3*A***). We confirmed *in vitro* phosphorylation of hENT2 by CKII using radiolabeled γ-[^{32}P]-ATP (Fig. 3*B*). Results also showed no phosphorylation of hENT2 by either PKA or PKC and no phosphorylation of hENT1 by CKII.

We further analyzed hENT1 and hENT2 *in vitro* phosphorylation by MS (Supplemental Figs. S2, 3) and confirmed hENT1 phosphorylation by PKA at Ser266, Ser269, Ser271, and Ser273 and hENT2 phosphorylation by CKII at Ser270, Ser282, and Thr285 (Fig. 3*A*). These results also corroborated no phosphorylation of hENT1 by either PKC or CKII, as well as no hENT2 phosphorylation by either PKA (positive phosphorylation of Ubq at Ser82) or PKC. Taken together, we confirmed that hENT1 is *in vitro* phosphorylated by PKA, whereas hENT2 is *in vitro* phosphorylated by CKII. These results suggest that hENT1 and hENT2 would be phosphorylated by 2 different kinases and that ENT PPI regulation would not be a result of direct phosphorylation by PKC.

PKC/PP1-dependent regulation disrupts hENT homomers and promotes formation of hENT heteromers at the plasma membrane

CKII is a constitutively active kinase, and regulation of CKII-phosphorylated proteins occurs as a result of the action of phosphatases (20, 21). Based on these facts, we hypothesized that PDD-dependent PKC activation would ultimately activate certain phosphatases subsequently to dephosphorylate hENT2 and trigger its traffic to the plasma membrane. To confirm this hypothesis, we performed a MYTH screen that identified PP1 as a potential PPI partner of hENT2.

To confirm the participation of PP1 in PKC-dependent regulation of hENTs, we further analyzed the formation of PPIs among hENTs in real time using the novel NanoBiT (**Fig. 4**) (17, 22). We confirmed the existence of PPI between hENT1–hENT1 (Fig. 4*A*), hENT1–hENT2 (Fig. 4*B*), and hENT2–hENT2 (Fig. 4*C*) in untreated HEK-293 cells. Coinciding with our previous results, PKC activation strikingly increased the number of hENT1–hENT2 heteromers and disrupted hENT1 homomers and hENT2 homomers. TTM-dependent PP1 inhibition showed no significant changes in the amount of hENT oligomers compared with untreated cells; however, PP1 inhibition reversed the effect of PKC activation (Fig. 4*B*). Therefore, we confirmed that PKC regulation of hENTs is PP1 dependent. Our results also suggest that PKC activation, together with PP1 participation, leads to disruption of hENT homomers and promotes formation of hENT heteromers.

Heteromerization of hENTs decreases hENT1-mediated uptake and increases hENT2-mediated uptake

We confirmed an increase in hENT2-mediated Hx uptake in HEK-293 cells after PKC activation (**Fig. 5*A***), coinciding with a previously observed increase in hENT2 presence at the plasma membrane. Interestingly, a hENT1-mediated 2-Cl-Ado uptake decreased after PKC activation (Fig. 5*B*). This effect was PP1 dependent (Fig. 5*C*). To confirm that regulation of hENT1 by PKC is a direct consequence of the

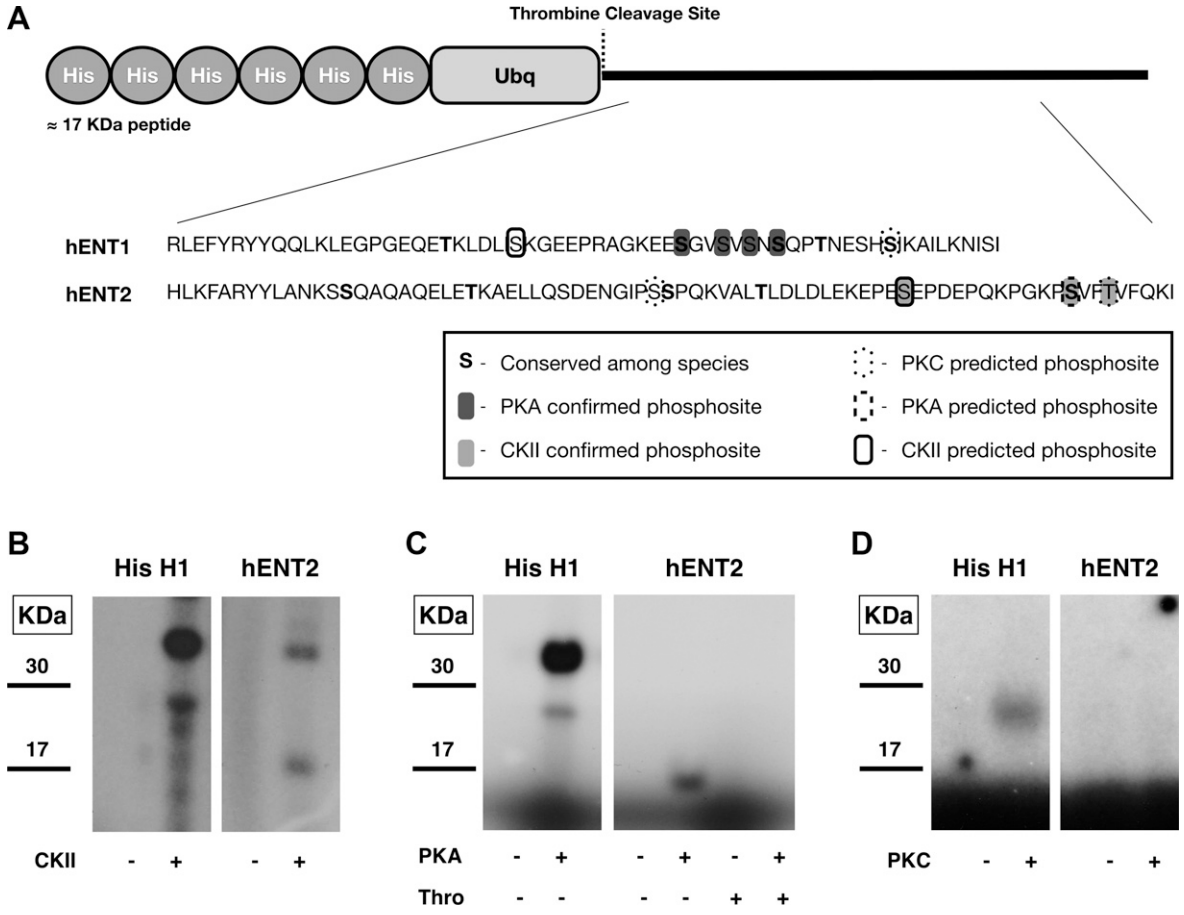

Figure 3. hENT1 and hENT2 can be phosphorylated by PKA and CKII, respectively, *in vitro*. *A*) Design and sequence of the constructs containing 6 residues of His, followed by Ubq, a thrombin cleavage site, and hENT1 or hENT2 intracellular loop. Circled residues are predicted phosphosites for PKC, PKA, or CKII, according to the *in silico* analysis using NetPhosK. Residues with gray background are phosphosites confirmed by MS for either PKA (dark gray) for hENT1 (Ser266, Ser269, Ser271, and Ser273) or CKII (light gray) for hENT2 (Ser270, Ser282, and Thr285) *in vitro*. MS results also showed no phosphorylation of hENT1 or hENT2 by PKC–only positive for histone H1 (Supplemental Figs. S2 and S3). *B*) Radiography of histone H1 (positive control) and hENT2-loop peptides after *in vitro* reaction with CKII. H1 showed a band above 30 kDa that belongs to the self-phosphorylated kinase (~40 kDa) and a band of ~22 kDa that belongs to H1. hENT2 was also positive for phosphorylation by CKII and showed a band at ~17 kDa. *C*) Radiography of H1 and hENT2-loop peptides after an *in vitro* reaction with PKA. Results showed 2 bands for H1, which belong to the self-phosphorylated kinase (~40 kDa) and H1 (~22 kDa). hENT2 was positive for phosphorylation by PKA when the peptide was intact but not after cleaving the 6×His-Ubq section with thrombin. These results suggest that Ubq is phosphorylated by PKA but not hENT2. These results were further confirmed by MS (Ubq phosphorylated at Ser82). *D*) Radiography of H1 and hENT2-loop peptides after an *in vitro* reaction with PKC. Results were positive for H1 (~22 kDa), but no phosphorylation was detected in the hENT2-loop. For the 3 panels, these are representative images of $n = 3$.

heteromerization between hENT1 and hENT2 (and not a direct effect of PKC on hENT1, independently of hENT2), we knocked down hENT2 protein expression (Fig. 5*D*), which resulted in decreased hENT2-mediated Hx uptake (Fig. 5*E*). Under these conditions, PKC activation did not result in decreased hENT1-related activity (Fig. 5*F*), thereby confirming that down-regulation of hENT1 by PKC activation is dependent on the presence of hENT2.

DISCUSSION

In this study, we are showing the existence of oligomers between hENT1 and hENT2 proteins. Oligomerization appears to be a novel mechanism of regulation of the biologic function of hENTs. Further studies are required to understand fully the regulatory effects between PKC and PP1 and how they trigger changes in subcellular locations of hENT2. Despite of the uncertainty of the mechanism involved, our study confirms PP1/PKC-dependent regulation of hENT2. Indeed, we propose a model for this type of mechanism that would involve homo- and hetero-oligomerization and traffic of hENT2 proteins to the plasma membrane after dephosphorylation by PP1 (**Fig. 6**). According to this model, hENT2 would be constitutively phosphorylated by CKII under basal conditions and localized at the submembrane area, where hENT2 proteins would reside as homomers. hENT1 is localized at the plasma membrane in the form of fully functional homomers. After PKC activation, PP1 dephosphorylates hENT2, resulting in its traffic to the plasma membrane, where hENT1–hENT2 PPIs would favor the formation of heteromers, while disrupting both hENT1 and hENT2 homomers. Those heteromers would translocate nucleobases, such as Hx, across

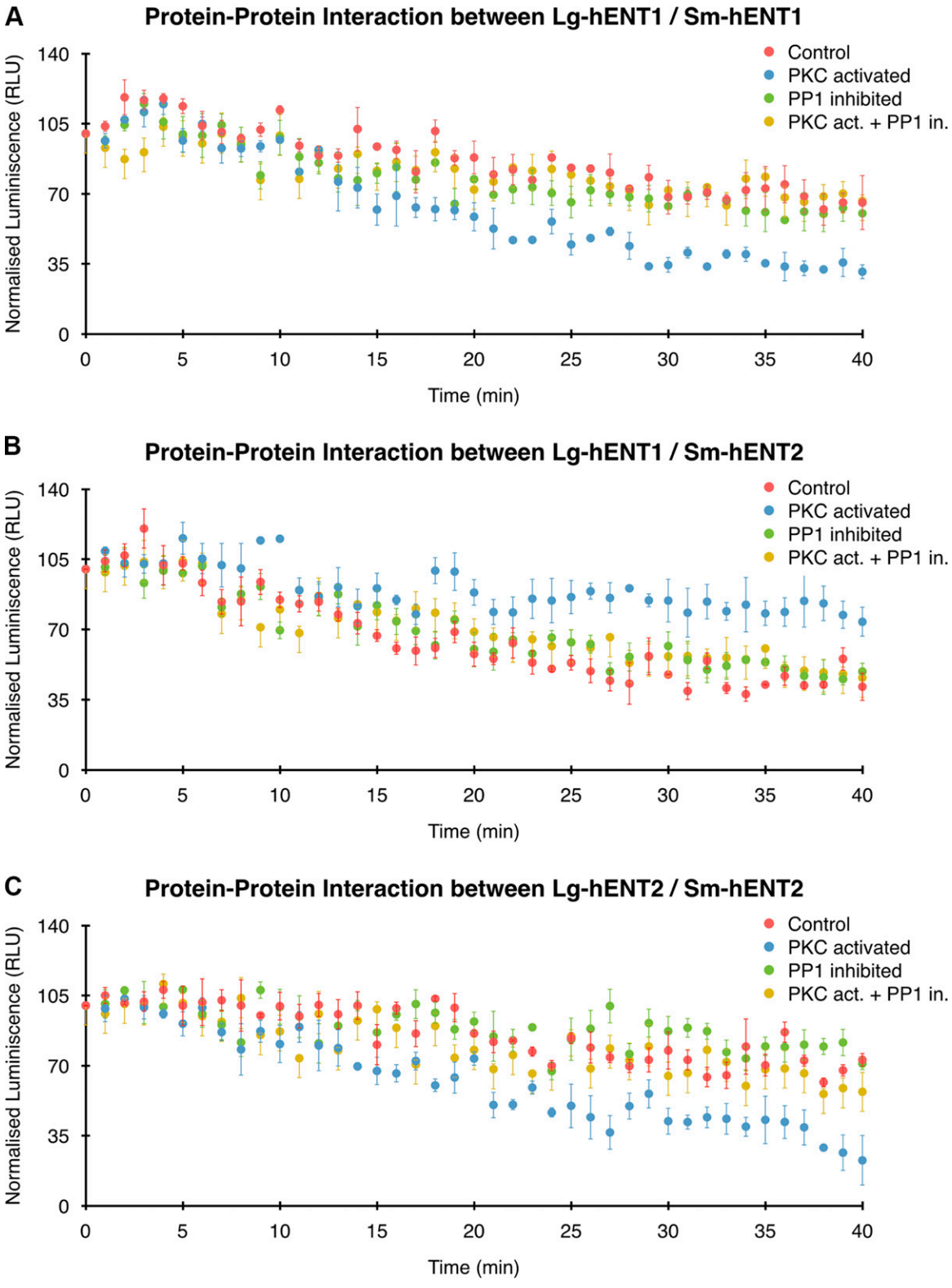

Figure 4. Changes in hENT oligomerization after PKC activation in HEK-293 cells are PP1 dependent. *A*) Existence of hENT1 homomers decreases after 10–15 min of PKC activation compared with untreated cells (control). *B*) Existence of hENT1–hENT2 heteromers increases after 10–15 min of PKC activation compared with untreated cells. *C*) Existence of hENT2 homomers decreases after 10–15 min of PKC activation. In all 3 panels, PP1 inhibited and PKC-activated plus PP1-inhibited cells showed no significant changes compared with control cells. These results confirmed that changes in hENT oligomerization after PKC activation are PP1 dependent. For the 3 panels, results show means ± SD; $n = 3$.

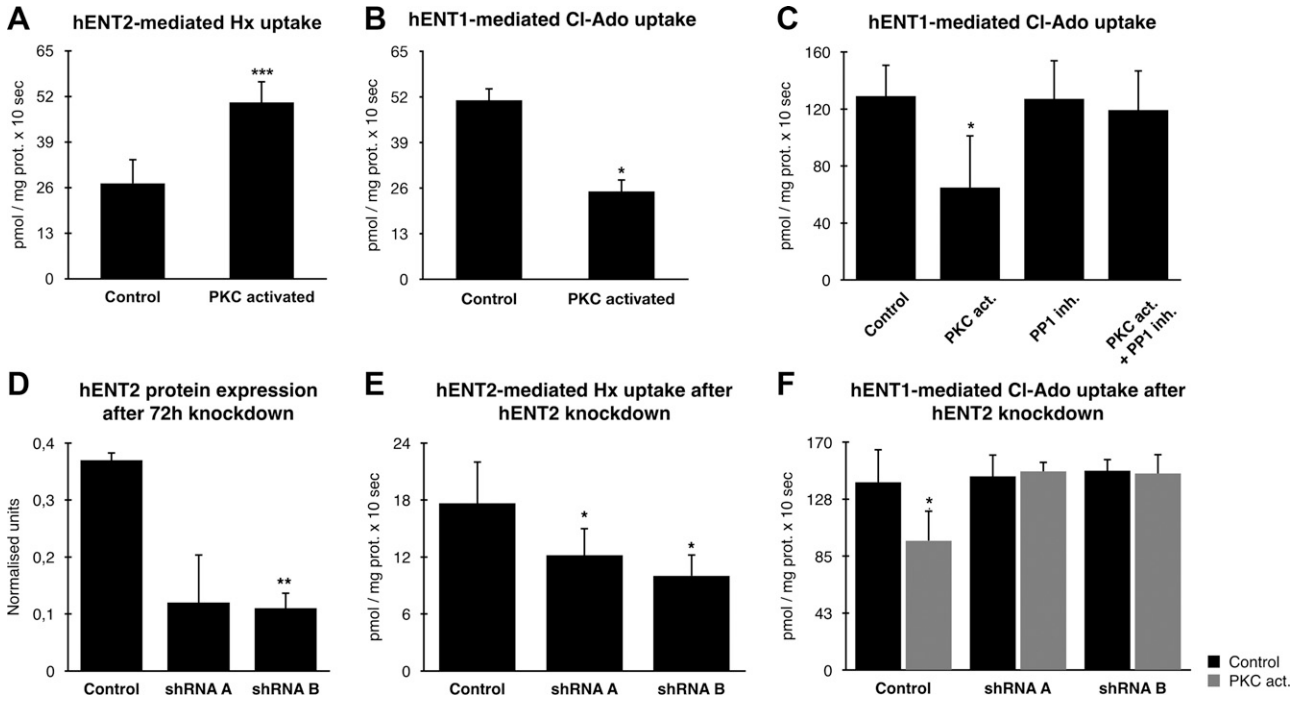

Figure 5. Oligomerization of hENTs regulates hENT-mediated uptake at the plasma membrane in HEK-293 cells. *A, B*) PKC activation significantly increases endogenous hENT2-mediated Hx uptake (*A*) and significantly decreases endogenous hENT1-mediated 2-Cl-Ado uptake (*B*). *C*) Down-regulation of endogenous hENT1 in PKC-activated cells did not occur when PP1 was inhibited simultaneously. These results confirm that hENT regulation by PKC is PP1 dependent. *D, E*) Knockdown of hENT2 mRNA after expression of short hairpin (sh)RNA A and shRNA B constructs leads to a significant decrease in endogenous hENT2 protein expression (*D*), as well as a significant decrease in endogenous hENT2-mediated Hx uptake (*E*). These results confirm the overall knockdown of hENT2 after 72 h of transfection. *F*) Down-regulation of endogenous hENT1 in PKC-activated cells did not occur in hENT2 knockdown cells. These results confirm that PKC regulation of hENT1 is hENT2-dependent. For all 6 panels, results show means ± SD; $n = 3$. $^*P < 0.05$, $^{**}P < 0.01$, $^{***}P < 0.001$.

the plasma membrane more efficiently than adenosine. Interestingly, in untreated cells, hENT2 appears to be located primarily below the plasma membrane (submembrane region), whereas hENT1 is located at the plasma membrane, both of them likely in the form of homomers. Consistent with our results, a previous study described disrupted plasma membrane localization of hENT2 in pancreatic cells, as hENT2 localized intracellularly along the submembrane area

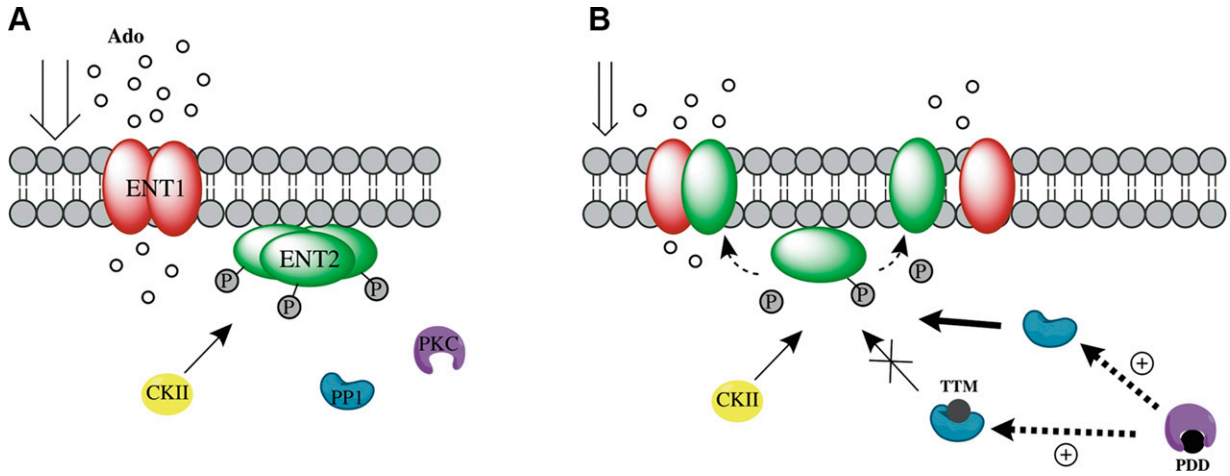

Figure 6. Proposed model for oligomerization of hENTs regulated by PKC and PP1 activation. *A*) In untreated cells, hENT1 is mostly located at the plasma membrane in the form of homomers and translocates 2-Cl-Ado to the cytosol. hENT2 is constitutively phosphorylated by CKII and is primarily located at the submembrane region in the form of homomers. *B*) After PKC activation, PP1 is activated and presumably dephosphorylates hENT2, which is trafficked to the plasma membrane. The presence of hENT2 at the plasma membrane disrupts hENT1 and hENT2 monomers and promotes the formation of hENT1 and hENT2 heteromers, which consequently, cause a decrease in hENT1-mediated 2-Cl-Ado uptake and an increase of hENT2-mediated Hx uptake.

(23). The occurrence of submembrane transporter populations likely to regulate transporter plasma membrane turnover may be, to some extent, novel for a nucleoside transporter, but it is not rare in transporter biology. Indeed, it has been previously described for other membrane proteins, such as ATP-binding cassette pumps, as well as potassium channels, among others (24–26). In most cases, the presence of such a population of vesicles in the submembrane space is related to a fast and finely tuned recycling/trafficking of the protein, which for sure, has significant impact on its biologic function. In this case, our findings suggest the possibility of a crosstalk among extracellular levels of adenosine, its metabolism, and transport processes (2, 27). Fast traffic of hENT proteins and changes in oligomerization partners would allow a fine modulation of adenosine removal but also of its extracellular catabolites, thereby contributing to adapt intracellular events to the anticipated oscillations of nucleoside and nucleobase concentrations likely to occur *in vivo*.

Furthermore, the data provided here confirm previous findings of phosphorylation of ENTs (2, 8, 19). We have confirmed the differential *in vitro* phosphorylation of hENT1 by PKA and hENT2 by CKII and identified the phosphorylated residues. Intriguingly, we observed no direct phosphorylation of hENT by PKC, despite the regulatory effects of the kinase corroborated by a pharmacological approach. Previous studies described contradictory effects of PKC activation on hENT1 and hENT2 regulation (28–31). We understand this disparity in the literature as a reflex of a complex and multicomponent mechanism of regulation that encompasses several kinases and phosphatases (32). Despite the central role of CKII in a large number of cellular signaling pathways, its own activity appears to be unregulated, as it is constitutively active. Thus, it has been suggested that changes in the phosphorylation status of CKII substrates, such as hENT2, would depend on regulated dephosphorylation (33). Although PKC-dependent PP1 activation and subsequent hENT2 dephosphorylation require further research, other proteins are known to be regulated by opposing effects of CKII and PP1 (34–36).

In summary, a novel mechanism of regulation of hENTs by oligomerization is proposed. This involves the formation of oligomers among hENT proteins in a way in which changes in the oligomeric status of hENT1 and hENT2 rapidly modify the uptake profile of nucleosides and nucleobases. The type of hENT oligomers formed is a consequence of changes in the subcellular localization of hENT2 proteins, which would ultimately be orchestrated by a complex network of kinase and phosphatase pathways. This opens the possibility of the adaptation of transport capacity to adenosine extracellular metabolism in a fast and finely tuned manner, which would be relevant to cell biology and pharmacology. FJ

ACKNOWLEDGMENTS

This work was supported by an Instituto de Salud Carlos III (Madrid, Spain), Predoctoral Contracts of Training in Health Research Doctoral Fellowship; a Ryerson University Postdoctoral Fellowship (to N.G.B.); Natural Science and Engineering Research Council of Canada; Ryerson University (to I.R.C.); Ministry of Economy and Competitiveness (National Biomedicine Program, Ministry of Economy, Industry and Competiveness); Government of Spain (SAF2014-52067-R); and National Biomedical Research Institute (CIBER) of Liver and Gastrointestinal Diseases (to M.P.-A.). CIBER is an initiative of Instituto de Salud Carlos III. The authors declare no conflicts of interest.

AUTHOR CONTRIBUTIONS

N. Grañe-Boladeras, D. Williams, M. Pastor-Anglada, and I. R. Coe designed research; N. Grañe-Boladeras and D. Williams analyzed data; N. Grañe-Boladeras, D. Williams, Z. Tarmakova, K. Stevanovic, and L. A. Villani performed research; N. Grañe-Boladeras, D. Williams, M. Pastor-Anglada, and I. R. Coe wrote the manuscript; and P. Mehrabi and K. W. M. Siu contributed new reagents or analytic tools.

REFERENCES

1. Cabrita, M. A., Baldwin, S. A., Young, J. D., and Cass, C. E. (2002) Molecular biology and regulation of nucleoside and nucleobase transporter proteins in eukaryotes and prokaryotes. *Biochem. Cell Biol.* **80**, 623–638
2. Dos Santos-Rodrigues, A., Grañé-Boladeras, N., Bicket, A., and Coe, I. R. (2014) Nucleoside transporters in the purinome. *Neurochem. Int.* **73**, 229–237
3. Baldwin, S. A., Beal, P. R., Yao, S. Y, King, A. E., Cass, C. E., and Young, J. D (2004) The equilibrative nucleoside transporter family, SLC29. *Pflugers Arch.* **447**, 735–743
4. Rose, J. B., Naydenova, Z., Bang, A., Eguchi, M., Sweeney, G., Choi, D ., Hammond, J. R., and Coe, I. R. (2010) Equilibrative nucleoside transporter 1 plays an essential role in cardioprotection. *Am. J. Physiol. Heart Circ. Physiol.* **298**, H771–H777
5. Löffler, M., Morote-Garcia, J. C., Eltzschig, S. A., Coe, I. R., and Eltzschig, H. K. (2007) Physiological roles of vascular nucleoside transporters. *Arterioscler. Thromb. Vasc. Biol.* **27**, 1004–1013
6. Ramakers, B. P., Riksen, N. P., Stal, T. H., Heemskerk, S., van den Broek, P., Peters, W. H, van der Hoeven, J. G., Smits, P., and Pickkers, P. (2011) Dipyridamole augments the antiinflammatory response during human endotoxemia. *Crit. Care* **15**, R289
7. Elsherbiny, N. M., Al-Gayyar, M. M, and Abd El Galil, K. H. (2015) Nephroprotective role of dipyridamole in diabetic nephropathy: effecte on inflammation and apoptosis. *Life Sci.* **143**, 8–17
8. Reyes, G., Nivillac, N. M, Karim, M. Z., Desouza, L., Siu, K. W. M., and Coe, I. R. (2011) The Equilibrative nucleoside transporter (ENT1) can be phosphorylated at multiple sites by PKC and PKA. *Mol. Membr. Biol.* **28**, 412–426
9. Bicket, A., and Coe, I. R. (2016) N-Linked glycosylation of N48 is required for equilibrative nucleoside transporter 1 (ENT1) function. *Biosci. Rep.* **36**, e00376
10. Ramadan, A., Naydenova, Z., Stevanovic, K., Rose, J. B., and Coe, I. R. (2014) The adenosine transporter, ENT1, in cardiomyocytes is sensitive to inhibition by ethanol in a kinase-dependent manner: implications for ethanol-dependent cardioprotection and nucleoside analog drug cytotoxicity. *Purinergic Signal.* **10**, 305–312
11. Bicket, A., Mehrabi, P., Naydenova, Z., Wong, V., Donaldson, L., Stagljar, I., and Coe, I. R. (2016) Novel regulation of equlibrative nucleoside transporter 1 (ENT1) by receptor-stimulated Ca2+-dependent calmodulin binding. *Am. J. Physiol. Cell Physiol.* **310**, C808–C820
12. Johnson, Z. L., Cheong, C. G., and Lee, S.Y. (2012) Crystal structure of a concentrative nucleoside transporter from Vibrio cholerae at 2.4 Å. *Nature* **483**, 489–493
13. Stecula, A., Schlessinger, A., Giacomini, K. M., and Sali, A. (2017) Human concentrative nucleoside transporter 3 (hCNT3, SLC28A3) forms a cyclic homotrimer. *Biochemistry* **56**, 3475–3483cntfch
14. Grañe-Boladeras, N.(2012) *Novel approaches to understanding hENT2 and hENT2-related proteins: from novel nuclear variants to global networks.* Ph.D. thesis, Universitat de Barcelona
15. Snider, J., Kittanakom, S., Damjanovic, D., Curak, J., Wong, V., and Stagljar, I. (2010) Detecting interactions with membrane proteins using a membrane two-hybrid assay in yeast. *Nat. Protoc.* **5**, 1281–1293

16. Blom, N., Sicheritz-Pontén, T., Gupta, R., Gammeltoft, S., and Brunak, S. (2004) Prediction of post-translational glycosylation and phosphorylation of proteins from the amino acid sequence. *Proteomics* **4**, 1633–1649
17. Dixon, A. S., Schwinn, M. K., Hall, M. P., Zimmerman, K., Otto, P., Lubben, T. H., Butler, B. L., Binkowski, B. F., Machleidt, T., Kirkland, T. A., Wood, M. G., Eggers, C. T., Encell, L. P., and Wood, K. V. (2016) NanoLuc complementation reporter optimized for accurate measurement of protein interactions in cells. *ACS Chem. Biol.* **11**, 400–408
18. Lu, G., Zhou, Q. X., Kang, S., Li, Q. L., Zhao, L. C., Chen, J. D., Sun, J. F., Cao, J., Wang, Y. J., Chen, J., Chen, X. Y., Zhong, D. F., Chi, Z. Q., Xu, L., and Liu, J. G. (2010) Chronic morphine treatment impaired hippocampal long-term potentiation and spatial memory via accumulation of extracellular adenosine acting on adenosine A1 receptors. *J. Neurosci.* **30**, 5058–5070
19. Coe, I., Zhang, Y., McKenzie, T., and Naydenova, Z. (2002) PKC regulation of the human equilibrative nucleoside transporter, hENT1. *FEBS Lett.* **517**, 201–205
20. Turowec, J. P., Duncan, J. S., French, A. C., Gyenis, L., St Denis, N. A., Vilk, G., and Litchfield, D. W. (2010) Protein kinase CK2 is a constitutively active enzyme that promotes cell survival: strategies to identify CK2 substrates and manipulate its activity in mammalian cells. *Methods Enzymol.* **484**, 471–493
21. Olsen, B. B., Guerra, B., Niefind, K., and Issinger, O. G. (2010) Structural basis of the constitutive activity of protein kinase CK2. *Methods Enzymol.* **484**, 515–529
22. Oh-Hashi, K., Hirata, Y., and Kiuchi, K. (2016) SOD1 dimerization monitoring using a novel split NanoLuc, NanoBit. *Cell Biochem. Funct.* **34**, 497–504
23. Nishio, R., Tsuchiya, H., Yasui, T., Matsuura, S., Kanki, K., Kurimasa, A., Hisatome, I., and Shiota, G. (2011) Disrupted plasma membrane localization of equilibrative nucleoside transporter 2 in the chemoresistance of human pancreatic cells to gemcitabine (dFdCyd). *Cancer Sci.* **102**, 622–629
24. Kipp, H., and Arias, I. M. (2002) Trafficking of canalicular ABC transporters in hepatocytes. *Annu. Rev. Physiol.* **64**, 595–608
25. Roma, M. G., Crocenzi, F. A., and Mottino, A. D. (2008) Dynamic localization of hepatocellular transporters in health and disease. *World J. Gastroenterol.* **14**, 6786–6801
26. Balse, E., El-Haou, S., Dillanian, G., Dauphin, A., Eldstrom, J., Fedida, D., Coulombe, A., and Hatem, S. N. (2009) Cholesterol modulates the recruitment of Kv1.5 channels from Rab11-associated recycling endosome in native atrial myocytes. *Proc. Natl. Acad. Sci. USA* **106**, 14681–14686
27. Longhi, M. S., Robson, S. C., Bernstein, S. H., Serra, S., and Deaglio, S. (2013) Biological functions of ecto-enzymes in regulating extracellular adenosine levels in neoplastic and inflammatory disease states. *J. Mol. Med. (Berl.)* **91**, 165–172
28. Delicado, E. G., Sen, R. P., and Miras-Portugal, M. T. (1991) Effects of phorbol esters and secretagogues on nitrobenzylthioinosine binding to nucleoside transporters and nucleoside uptake in cultured chromaffin cells. *Biochem. J.* **279**, 651–655
29. Sen, R. P., Delicado, E. G., and Miras-Portugal, M. T. (1999) Differential modulation of nucleoside transport types in neuroblastoma cells by protein kinase activation. *Neuropharmacology* **38**, 1009–1015
30. Montecinos, V. P., Aguayo, C., Flores, C., Wyatt, A. W., Pearson, J. D., Mann, G. E., and Sobrevia, L. (2000) Regulation of adenosine transport by D-glucose in human fetal endothelial cells: involvement of nitric oxide, protein kinase C and mitogen-activated protein kinase. *J. Physiol.* **529**, 777–790
31. Pinto-Duarte, A., Coelho, J. E., Cunha, R. A., Ribeiro, J. A., and Sebastião, A. M. (2005) Adenosine A2A receptors control the extracellular levels of adenosine through modulation of nucleoside transporters activity in the rat hippocampus. *J. Neurochem.* **93**, 595–604
32. Weber, S., Meyer-Roxlau, S., and El-Armouche, A. (2016) Role of protein phosphatase inhibitor-1 in cardiac beta adrenergic pathway. **101**, 116–126
33. Pinna, L. A. (1990) Casein kinase 2: an 'eminence grise' in cellular regulation? *Biochim. Biophys. Acta* **1054**, 267–284
34. Zhang, S., and Kim, K. H. (1997) Protein kinase CK2 down-regulates glucose-activated expression of the acetyl-CoA carboxylase gene. *Arch. Biochem. Biophys.* **338**, 227–232
35. Wang, H., Song, C., Gurel, Z., Song, N., Ma, J., Ouyang, H., Lai, L., Payne, K. J., and Dovat, S. (2014) Protein phosphatase 1 (PP1) and casein kinase II (CK2) regulate Ikaros-mediated repression of TdT in thymocytes and T-cell leukemia. *Pediatr. Blood Cancer* **61**, 2230–2235
36. Watabe, M., and Nakaki, T. (2011) Protein kinase CK2 regulates the formation and clearance of aggresomes in response to stress. *J. Cell Sci.* **124**, 1519–1532

Received for publication March 8, 2018.
Accepted for publication November 5, 2018.